Nucl. Sci. and Tech., Vol.11, No. 4 (2021), pp. 07-18

Nuclear Science and Technology

Journal homepage: http://jnst.vn/index.php/nst

Performance Comparison of ANN-Based Model and Empirical Correlations for Void Fraction Prediction of Subcooled Boiling Flow in Vertical Upward Channel

Ngoc Dat Nguyen, Van Thai Nguyen*

Department of Nuclear Engineering and Environmental Physics, School of Engineering Physics, Hanoi University of Science and Technology (HUST)
**E-mail: thai.nguyenvan@hust.edu.vn*

Abstract: The accurate prediction of void fraction parameter in subcooled boiling flow is very important for nuclear safety since it has significant influences on the mass flow rate, the onset of two-phase flow instability, and the heat transfer characteristics in a nuclear reactor core. Many different models and empirical correlations have been established over a variety of input conditions; however, this classical approach could lead to unsatisfactory prediction due to the uncertainties of model parameter and model forms. To cope with these limitations, Artificial Neural Network (ANN) is a powerful machine learning tool for modeling and solving non-linear and complicated physical problems. Therefore, this work is aim at developing an ANN-based model to predict the local void fraction of subcooled boiling flows. The comparison results of the performance between the ANN-based model and empirical correlations for the void fraction prediction of subcooled boiling in vertical upward channel showed the potential use of ANN-based model in the Computational Fluid Dynamics (CFD) codes to accurately simulate the subcooled boiling phenomena.

Keywords: *Subcooled Boiling, Void fraction, Artificial Neural Network.*

I. INTRODUCTION

Subcooled boiling flow have become challenging issues in safety analysis of water-cooled nuclear power reactors since the physical-mechanisms of void growth and related thermal-hydraulic behaviors of system are still not fully understood. In particular, accurate prediction of void fraction parameter in subchannels under two-phase flow conditions is of great importance to the nuclear safety analysis. Thermal-hydraulic system codes and *Computational Fluid Dynamic* (CFD) solvers have been widely recognized as promising tools for dealing with the thermal-hydraulic phenomena simulating transients and accident scenarios in nuclear power plant. However, a lot of constitutive models and correlations are required to implement in these codes to make the conservation equations solvable. This classical approach could lead to unsatisfactory prediction due to the uncertainties of model parameter and model forms [1].

The *Artificial Neural Network* (ANN) is a powerful machine learning tool for modeling and solving non-linear and complicated physical problems, and it can be applied to overcome above-mentioned limitations. Many investiga-tors proposed ANN-based model to predict the void fraction, flow pattern, pressure drop and heat transfer coefficient, demonstrating the predictive capability of the model [2-5]. Currently, no research has been

https://doi.org/10.53747/nst.v11i4.335
Received 28 March 2022, accepted 21 June 2022

conducted to check the performance and applicability of the ANN-based model and the empirical correlations for the subcooled boiling void fraction prediction problem in vertical upward channel. Therefore, in this study, comparison study is considered and investigated, proceeding to use the ANN-based model to replace the empirical correlations in the thermal-hydraulics codes.

Nomenclature

b	Parameter defined in Eq. 10
C	Distribution parameter
C_1, C_2, C_3	Parameter defined in Eq. 11
c_p	Specific heat at constant pressure
D_h	Hydraulic diameter
f	Fitness function
G	Mass flux
g	Gravity
h	Enthalpy
h_{fg}	Laten heat of vaporization
k	Thermal conductivity
MAE	Mean Absolute Error
MSE	Mean Square Error
n	Number of datapoints
NWB	Number of weights and biases
Pe	Peclet number
Pr	Prandtl number
p	Pressure
q''	Heat flux
Re	Reynolds number
R^2	Coefficient of determination
R_{cr}	Crossover rate
R_{mt}	Mutation rate
S	Slip ratio
T	Temperature
u	Velocity
u^*	Parameter defined in …
u_{gj}	Drift velocity
z	Distance from tube inlet

Greek symbols

α	Void fraction
μ	Viscosity
ρ	Density
σ	Surface tension
χ	Flow quality
χ_e	Thermodynamic equilibrium quality

Subscripts

exp	Experimental (measured)
f	Liquid
g	Vapor/gas
H	Homogenous model
in	Inlet
nvg	Net vapor generation
$pred$	Predicted
sat	Saturated
sub	Subcooling
$train$	Training data
$test$	Testing data

II. FUNDAMENTALS AND EXPERIMENTS OF SUBCOOLED BOILING FLOW

A. Void fraction in subcooled boiling flow

Knowledge of void fraction in subcooled flow boiling is of considerable practical importance because it is indispensable to the prediction of several other two-phase parameters, such as thermophysical properties, pressure drops

heat transfer coefficient, and critical heat flux. Moreover, void fraction plays a crucial role when characterizing flow regime transitions in subcooled flow boiling [6]. Subcooled boiling flow is influenced by several factors, including inlet pressure, inlet subcooling, mass flux, heat flux, flow orientation, tube shape and hydraulic diameter as well as thermophysical properties of the working fluid. The lack of thermodynamic equilibrium between the vapor and liquid phases is the main reason which causes great difficulty of modeling interfacial behavior and predicting void fraction in subcooled boiling.

Subcooled boiling flow is initiated with a single-phase liquid region at the inlet wherein the mean liquid temperature increases gradually in the axial direction in response to an applied heat flux. Using the commonly adopted assumption of thermodynamic equilibrium, vapor is postulated to begin forming at the axial location from the inlet corresponding to zero thermodynamic equilibrium quality (χ_e). However, in practical terms, the vapor will begin forming upstream of this location despite the bulk liquid remaining below saturation temperature, provided the wall temperature sufficiently exceeds the saturation temperature to permit vapor formation at the wall. The location where the first bubbles appear is the point of *Onset of Nucleate Boiling* (ONB), but, in highly subcooled boiling, the region immediately following ONB does not contribute any appreciable increase in vapor void fraction, given that bubbles in this region are subjected to a high degree of condensation. Farther downstream, as the bulk liquid temperature continues to rise to saturation temperature, which weakens the condensation effects, causing the wall bubbles to grow bigger and begin departing into the bulk flow, thereby allowing for a significant increase in void fraction. The axial location where the void fraction begins to incur such an increase is referred to as point of *Net Vapor Generation* (NVG). A common demarcation of subcooled boiling flow region is: (i) single-phase liquid region upstream of the location of ONB, (ii) two-phase highly subcooled region between the axial locations of ONB and NVG, (iii) slightly subcooled region between the axial locations of NVG and $\chi_e = 0$, and (iv) saturated boiling region beginning at the location of $\chi_e = 0$. Clearly, the void fraction trend varies greatly among these regions.

B. Consolidated database for subcooled boiling in vertical upward channel

Due to the complexity of the phenomena, the experimental studies have been the main research approach to develop empirical correlations and models which provide the engineers and designers suitable choice in engineering practice. In this study, the experiment data of void fraction distribution performed by previous studies [7-17] in cylindrical and annular vertical channels were used to assess the correctness accuracy of typical empirical correlations and the ANN-based model. The collected database including 308 cases (a total of 2016 data points) are listed in Table I with main parameters such as hydraulic diameter (D_h), heating section length (L_{heated}), uniform heat flux (q''), inlet pressure (p_{in}), inlet subcooling ($\Delta T_{sub,in}$), and mass flux (G).

Table I. The database of subcooled boiling in vertical upward channels

Author(s)	D_h (mm)	L_{heated} (m)	q'' (kW/m^2)	G (kg/m^2-s)	$\Delta T_{sub,in}$ (K)	p_{in} (bar)
Ferrell (1964) [7]	11.84	2.44	230 – 682	134 – 1785	28 – 126	4 – 17
Rouhani (1966) [8]	13.00	1.09	600 – 1220	121 – 1445	6 – 150	9 – 50
Zeitoun (1994) [9]	12.70	0.30	207 – 705	139 – 412	12 – 31	1 – 1.7
Devkin (1998) [10]	10 – 12	0.4 – 1.5	132 – 2210	126 – 2123	4 – 171	11 – 150
Situ et al (2004) [11]	19.1	1.73	98 – 151	475 – 1181	8 – 13	1.26 – 1.36
Lee et al (2009) [12]	19.1	1.73	50 – 193	481 – 1939	8 – 15	1.32 – 1.48
SUBO (2010) [13,14]	25.52	3.1	364 – 568	1104 – 2129	17 – 30	1.8 – 2.0
Lee et al (2012) [15]	18.5	1.61	133 – 320	476 – 1061	12 – 21	1.15 – 1.6
Ozar et al (2013) [16]	19.1	2.8	109 – 241	445 – 1844	10 – 28	2.2 – 9.5
Brooks et al (2014) [17]	19.1	2.85	241 – 264	933 – 957	13 – 15	3.3 – 5.0
Overall	**11.84 – 25.52**	**0.3 – 3.1**	**50 – 2210**	**121 – 2129**	**4 – 171**	**1 - 150**

III. PREDICTIVE METHODS FOR VOID FRACTION IN SUBCOOLED BOILING FLOW

A. Predictive method using empirical correlations

Due to the complexity in treating thermo-dynamic non-equilibrium effects, prediction of void fraction in a purely theoretical manner is a formidable challenge. Therefore, most published void fraction relations follow purely empirical or semi-empirical formulations, relying heavily on idealizations of underlying interfacial behavior and fitting of empirical coefficients. The use of empirical correlations is very complex and requires the application of many different formulas. This section presents typical models often used in the problem of predicting the void fraction of subcooled boiling flows. All thermophysical properties of the working fluids are obtained from NIST's REFPROP software. The calculation process of void fraction is proposed by *Cai et al. (2021)* [6], including the steps below.

(1) Input the inlet condition parameters, such as p_{in}, D_h, G, $\Delta T_{sub,in}$ and q'', and then calculate the axial distribution of thermodynamic equilibrium quality χ_e, using Eq. (1).

(2) Calculate thermodynamic equilibrium quality at the NVG point $\chi_{e,nvg}$, using the different correlations. If the calculated $\chi_{e,nvg}$ is less than $\chi_{e,in}$, $\chi_{e,nvg}$ is substituted by the value of $\chi_{e,in}$.

(3) Calculate the axial distribution of vapor quality χ which is a function of both $\chi_{e,nvg}$ and χ_e, using the different correlations.

(4) Calculate the axial distribution of void fraction α, using the different correlations.

A useful reference for exploring two-phase behavior in subcooled boiling is local thermodynamic equilibrium quality, which is defined as Eq. (1). In a uniformly heated vertical channel, this parameter can be calculated using a simple energy balance.

$$\chi_e = \frac{h - h_{f,sat}}{h_{fg}} = \frac{\frac{4q''z}{GD_h} + h_{in} - h_{f,sat}}{h_{fg}} \quad (1)$$

Where h_{in}, q'', G, D_h and z are, respectively, the liquid inlet enthalpy, wall heat flux, mass flux, hydraulic diameter, and axial distance from the inlet.

Following the mechanisms of bubble departure and bubble ejection form the heated wall, *Dix (1971)* [18] proposed a mechanism relating the occurrence of the NVG point, indicating that this is the location where there is a high probability of bubble leaving the wall, leading to an increase in significant of void fraction parameter. Therefore, research models aimed at predicting the position of the NVG point as well as determining the corresponding $\chi_e = \chi_{(e,nvg)}$, which is of great important in predicting the void fraction. In this study, two empirical correlations of NVG point are the models of *Saha and Zuber (1974)* [19] and *Ha et al. (2020)* [20] used to calculate $\chi_{e,nvg}$.

Saha and Zuber (1974) [19]

$$\chi_{e,nvg} = \begin{cases} -0.0022\dfrac{q'' c_{pf} D_h}{h_{fg} k_f}, Pe < 70000 \\ -153.85\dfrac{q''}{h_{fg} G} \quad , Pe \geq 70000 \end{cases} \tag{2}$$

$$Pe = \frac{G.D_h.c_{pf}}{k_f}$$

Ha et al. (2020) [20]

$$\chi_{e.nvg} = \begin{cases} -\dfrac{q'' c_{pf} D_h}{h_{fg} k_f}\left[0.0901 - 0.0893\exp\left(-\dfrac{158}{Pe}\right)\right. \\ -\dfrac{q'' c_{pf} D_h}{h_{fg} k_f}\dfrac{Re^{-0.77} Pr^{-1.35}}{0.0959} \end{cases}$$

$$u^* = \frac{G}{1.53\rho_f}\left[\frac{\rho_f^2}{g\sigma(\rho_f - \rho_g)}\right]^{0.25} \tag{3}$$

In calculating vapor quality χ, the method of *Saha and Zuber (1974)* [19] has been shown to yield physically acceptable values across broad ranges of conditions. Therefore, Saha & Zuber's model (Eq. 4) is selected for ultimate calculation of the void fraction.

$$\chi = \frac{\chi_e - \chi_{e,nvg}\exp(\chi_e/\chi_{e,nvg} - 1)}{1 - \chi_{e,nvg}\exp(\chi_e/\chi_{e,nvg} - 1)} \tag{4}$$

The paper includes three categories of void fraction prediction methods: (1) homogeneous flow model (HM), (2) slip ratio model, (3) drift-flux model. Combining the definitions of void fraction and vapor quality yields the following relation for one-dimensional (slip) two-phase flow:

$$\alpha = \frac{1}{1 + S\dfrac{1-\chi}{\chi}\dfrac{\rho_g}{\rho_f}} \tag{5}$$

Where the slip ratio $S = u_g/u_f$ is the ratio between the vapor and liquid velocity. Eq. (5) can be simplified in a HM model where $S = 1$.

$$\alpha_H = \frac{1}{1 + \dfrac{1-\chi}{\chi}\dfrac{\rho_g}{\rho_f}} \tag{6}$$

In this study, the slip ratio model of *Ahmad (1970)* [21] and *Cai et al (2021)* [6] are used to calculate void fraction.

Ahmad (1970) [21]

$$\alpha = \frac{1}{1 + \dfrac{1-\chi}{\chi}\left(\dfrac{GD_h}{\mu_f}\right)^{-0.016}\left(\dfrac{\rho_g}{\rho_f}\right)^{0.795}} \tag{7}$$

Cai et al. (2021) [6]

$$\alpha = \frac{1}{1 + \dfrac{1-\chi}{\chi}\left(\dfrac{\rho_g}{\rho_f}\right)^{0.7988}} \tag{8}$$

Zuber and Findlay (1965) [22] proposed general framework for the drift-flux model to determine void fraction according to the relation Eq. (9)

$$\alpha = \frac{\chi}{C\left[\chi + \dfrac{\rho_g}{\rho_f}(1-\chi)\right] + \dfrac{\rho_g u_{gj}}{G}} \tag{9}$$

Where C is termed distribution parameter and u_{gj} is drift velocity, which can be determined through various correlations. In this study, the drift-flux model of *Dix (1971)* [18] is utilized, detailed in Eq. (10).

$$C = \frac{\chi\rho_f}{\chi\rho_f + (1-\chi)\rho_g}\left[1 + \frac{(1-\chi)\rho_g}{\chi\rho_f}\right]^b$$

$$b = \left(\frac{\rho_f}{\rho_g}\right)^{0.1} \quad (10)$$

$$u_{gj} = 2.9\left[\frac{g\sigma(\rho_f - \rho_g)}{\rho_f^2}\right]^{0.25}$$

B. Predictive method using ANN-based model

With ANN approach, experimental databases are used in the training process in which the weights and biases are modified to attain better approximation of the desired output. The subcooled boiling flow phenomena are primarily governed by the flow boundary conditions as well as the geometry of the flow domain, therefore these key parameters must be selected as inputs for ANN structure design and optimization. The input parameters of ANN for prediction of two-phase flow parameters can be chosen based on general understanding and conventional empirical correlations [23]. Fundamentally, the prediction of void fraction was based on the drift-flux model, in which the liquid superficial velocity, gas superficial velocity, hydraulic diameter of channel, and pressure were generally considered as the related correlating parameters [24]. Therefore, Five key parameters of flow boundary conditions including hydraulic diameter (D_h), mass flux (G), heat flux (q''), inlet subcooling $\Delta T_{sub,in}$, and inlet pressure (p_{in}) are chosen as input variables of ANN. Additionally, one variable indicating the location of measured points are the axial length (L/D_h: the ratio between the flow length from the inlet of heated section L and the hydraulic diameter D_h) is also chosen as input of ANN structure.

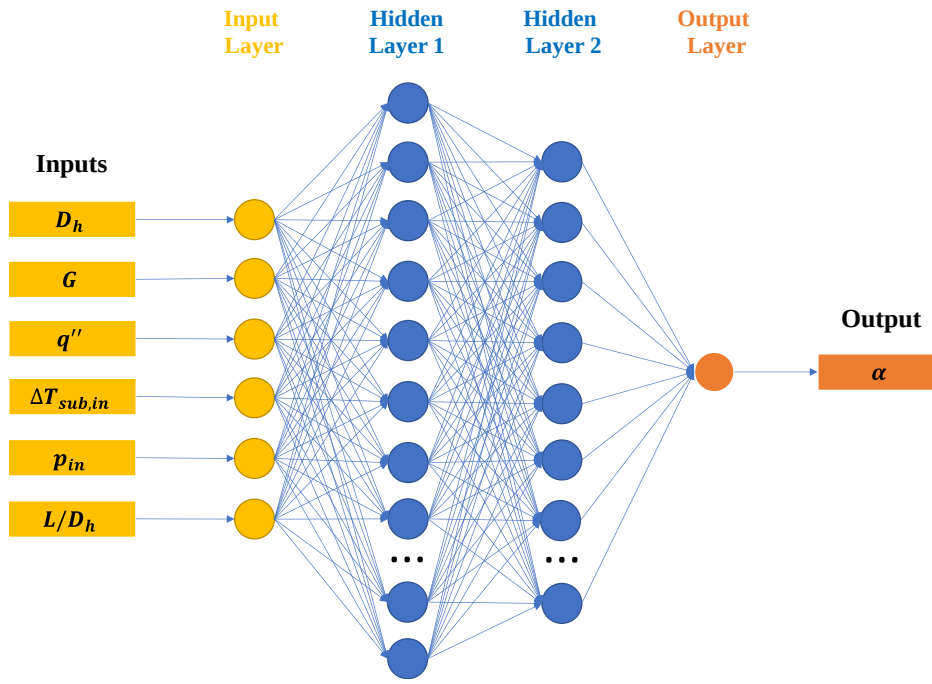

Fig. 1. Structure of ANN-based model

The type of ANN used in this work is the *multilayer feedforward net*, including one input layer, one output layer, and two hidden layers (Fig. 1). The number of neurons in input and output layer are determined based on six input parameters and one predicted parameter (void fraction). To determine the number of neurons in each hidden layer, the *Genetic Algorithm* (GA) is utilized to optimize the ANN structure [24]. To apply GA for ANN structural optimization, each ANN structure (the number of neurons at each hidden layer) is considered as an individual with corresponding chromosome made up of many genes which are represented using a string with binary values (string of 1s and 0s). This study adopted chromosome coding scheme proposed by *Benardos and Vosniakos (2007)* [25] with a 2x6 bits binary chromosome in which the first and second group of 6 bits correspond to number neurons in the first and second hidden layer, respectively (see Fig. 2). The population size, number of generations, crossover rate and mutation rate are important control parameters which directly influence the ability to search an optimum solution in Genetic Algorithm. The control parameters used in this study are presented in Table II based on a comprehensive survey.

The chromosome coding scheme											
Part 1: The first hidden layer						**Part 2**: The second hidden layer					
1	**1**	**1**	**1**	**1**	**1**	**0**	**1**	**0**	**0**	**1**	**0**
$2^5 + 2^4 + 2^3 + 2^2 + 2^1 + 2^0 = \mathbf{63}$						$2^4 + 2^1 = \mathbf{18}$					

Fig. 2. An example of the coding scheme of 12-bit chromosome

Table II. The control parameters used in GA

Population sizes	Number of generations	Crossover rate	Mutation rate
30	10	90%	5%

With ANN structural optimization framework [24] using GA, a population with thirty different ANN structures (individuals) is randomly initialized and these structures are trained in turn on the same database with the same training conditions. During training process, the fitness values (Eq. 11) will be calculated based on the method of *Nguyen and Nguyen (2022)* [24], and the corresponding weights and biases are saved. After the end of each generation, the selection of better individuals will be decided on the smaller fitness value. Two good individuals are randomly selected for crossover to produce two offspring with the crossover rate R_{cr} = 0.9, and the mutation rate R_{mt} = 0.05. Two offspring were assessed for fitness values and replaced less well-adapted individuals in the population. The GA process ends when all ten generations have been completed and the best individual in each generation are compared to select the final one. The GA process are then repeated several times to produce the best individual in each process and the second round of selection will be done based on smallest fitness value.

$$f = e^{0.005 \times NWB} \times (1 + 0.33C_1 + C_2 + C_3) \times \frac{MSE_{train} n_{train} + MSE_{test} n_{test}}{n_{train} + n_{test}} \quad (11)$$

Where NWB is the total number of weights and biases, C_1, C_2 is the number of test cases where the absolute value of relative

error is in the internal [15,25], [25,∞], respectively. C_3 is the number of test case where the value of predicted result lying outside the range of target value. In optimization process, the predicted results by the ANN-based model are compared with target value through mean square error (*MSE*) (Eq. 12).

$$MSE = \frac{\sum_i \left(\alpha_{i,pred} - \alpha_{i,exp}\right)^2}{n} \quad (12)$$

Where $\alpha_{i,pred}$ and $\alpha_{i,exp}$ are, respectively, predicted, and measured values, n is a total of data points.

The database including 2016 data points, after pre-processing is divided into three parts: 70% is used for training, 20% is used for testing and 10% for validation [24]. Each ANN configuration has its weights and biases initialized using the *Nguyen-Widrow* method. To avoid *overfitting*, the ANN is trained with the *Levenberg-Marquardt* along with *early stopping*.

After the optimization process, the best ANN is used to predict void fraction parameter based on six input parameters. In other works, the ANN has constructed a model, in which void fraction is a function of six input variables through the matrixes of weight and bias.

IV. RESULTS AND DISCUSSION

The results calculated by the ANN-based model and the empirical correlations are compared with the corresponding measured values through the *Mean Absolute Error* (MAE) defined by Eq (13). The MAE values of the models used in the study are presented in Table II. Fig. 3 shows the comparison between the values predicted by several models with the experimental measurements. In addition, the coefficient of determination (R^2) is used to evaluate the linear regression of the ANN-based model, whereby the closer the value of R is to 1, the more predictive the model is good. The correlation coefficient R^2 (Eq. 14) is determined on the test data set (R_{test}) to evaluate the generality of the model and on the all-data (R_{all}) to evaluate the predictive ability of the model over all-data. The results are presented in Fig. 4.

$$MAE = \frac{1}{n}\sum_i \left|\alpha_{i,pred} - \alpha_{i,exp}\right| \quad (13)$$

$$R^2 = 1 - \frac{\sum_i \left(\alpha_{i,pred} - \alpha_{i,exp}\right)^2}{\sum_i \left(\alpha_{i,exp} - \alpha_{mean}\right)^2} \quad (14)$$

It can be seen in Table III that the void fraction prediction model of *Cai et al (2021)* [6] gives the most accuracy among the investigated correlations, this has also been shown in the author's research [6]. Besides, the use of the model of *Saha and Zuber (1974)* [19] to calculate the thermodynamic equilibrium quality at the NVG point is more effective than to use the model of *Ha et al (2020)* [20]. Most of the above empirical correlation models can predict relatively accurately for the data set of *Ferrell (1964)* [7] and *Devkin (1998)* [10] because these are common data sets, often used to develop the above correlation models. For other data, there exists a significant difference when using empirical correlations for prediction. Especially, in the low range of void fractions, the inaccurate prediction results show the limitation of using empirical correlation models.

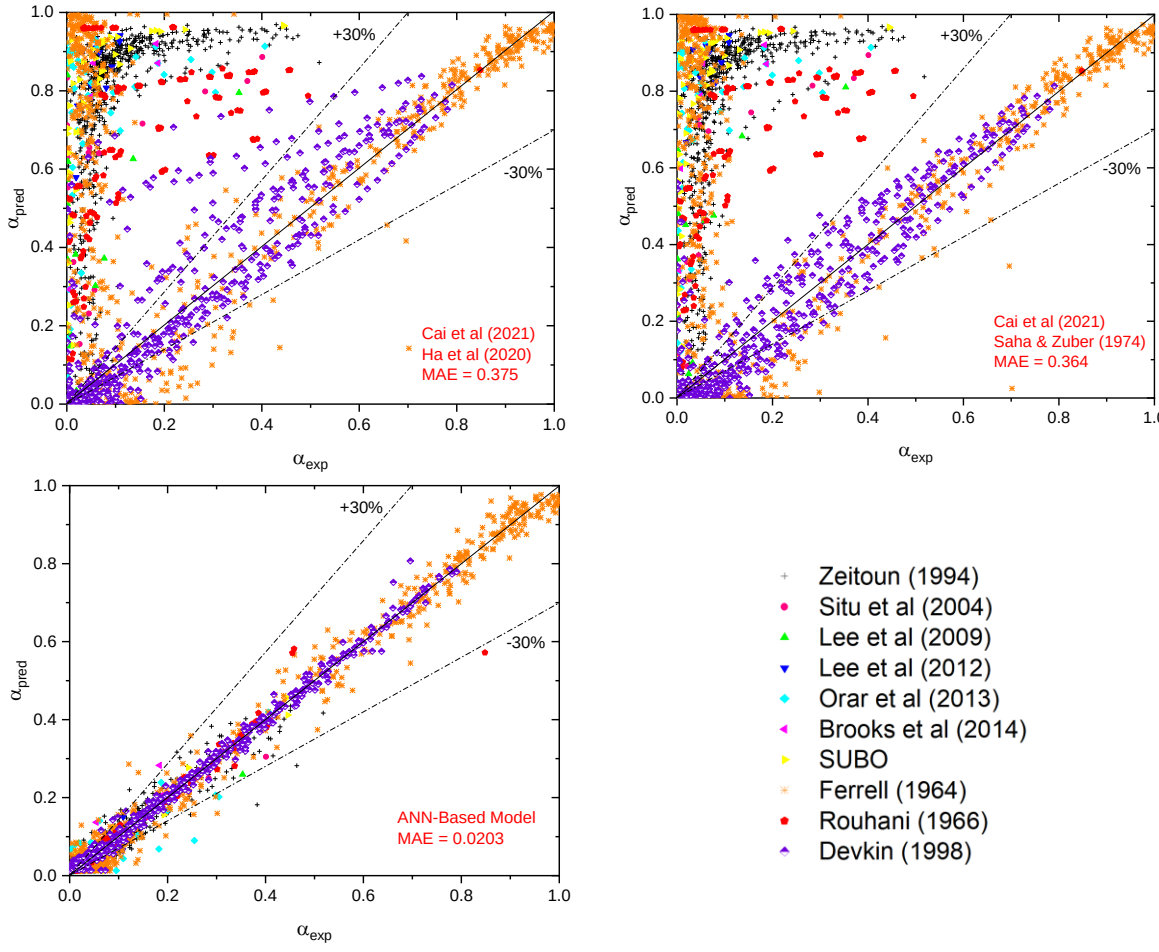

Fig. 3. Comparison of experimental data with predicted results

Based on the value of the MAE as well as the comparison results presented in Fig. 3, it can be easily seen that the predictive performance of the ANN-based model is superior to the above empirical correlation models. The ANN-based model also overcomes the limitation in predicting low void fraction values. That demonstrates the potential of using ANN-based model to replace previous traditional empirical correlations.

At high pressure ranges and/or inlet subcooling, the void fraction along the chanel is very complicated. In this work, the distribution of experimental data according to inlet pressure and inlet subcooling is presented in Fig. 5. Due to limited experimental data available in previous publications, especially data in the high pressure ranges so the database used in this study is mainly in the low pressure range from 1 to 10 bar. The number of data points is concentrated mainly in the inlet subcooling range from 10 to 30 K. The performance of ANN-based model depends not only on the availability of the databases, but also on the concentration of data points in each input parameter [23].Therefore, the ANN-based model developed in this study will work efficiently in the low pressure range (1-10 bar) and inlet subcooling range from 10 to 30 K.

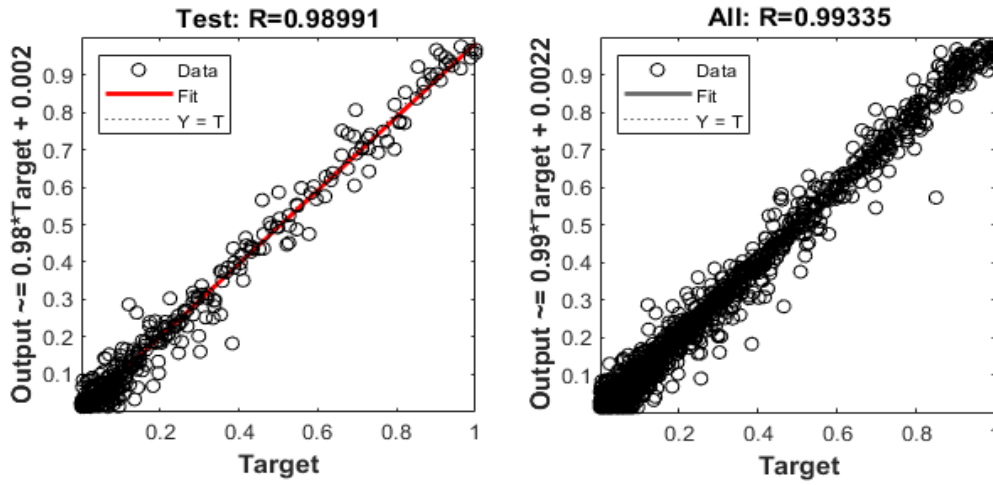

Fig. 4. Comparison of experimental data with predicted results for test data and all-data (ANN-based model)

Table III. Mean absolute errors of 8 empirical correlation models and ANN-based model against experimental data

Author(s)		Overall, MAE	Ferrell 1964	Rouhani 1966	Zeitoun 1994	Devkin 1998	Situ 2004	Lee 2009	SUBO 2010	Lee 2012	Ozar 2013	Brooks 2014
$\chi_{e,nvg}$	α											
Saha&Zuber	**HM**	0.473	0.394	0.497	0.737	0.134	0.526	0.433	0.712	0.879	0.725	0.770
Saha&Zuber	**Ahmad**	0.375	0.312	0.523	0.605	0.078	0.317	0.240	0.569	0.763	0.600	0.625
Saha&Zuber	**Dix**	0.369	0.316	0.507	0.593	0.057	0.339	0.266	0.600	0.800	0.612	0.650
Saha&Zuber	**Cai**	0.364	0.309	0.494	0.589	0.071	0.293	0.218	0.545	0.742	0.576	0.598
Ha	**HM**	0.485	0.385	0.626	0.769	0.155	0.548	0.473	0.697	0.869	0.725	0.759
Ha	**Ahmad**	0.387	0.299	0.527	0.639	0.097	0.357	0.274	0.558	0.741	0.599	0.613
Ha	**Dix**	0.380	0.302	0512	0.628	0.075	0.387	0.303	0.589	0.779	0.612	0.636
Ha	**Cai**	0.375	0.295	0.499	0.623	0.087	0.337	0.251	0.535	0.719	0.574	0.585
ANN-based model		**0.020**	**0.027**	**0.013**	**0.020**	**0.012**	**0.016**	**0.021**	**0.017**	**0.019**	**0.034**	**0.036**

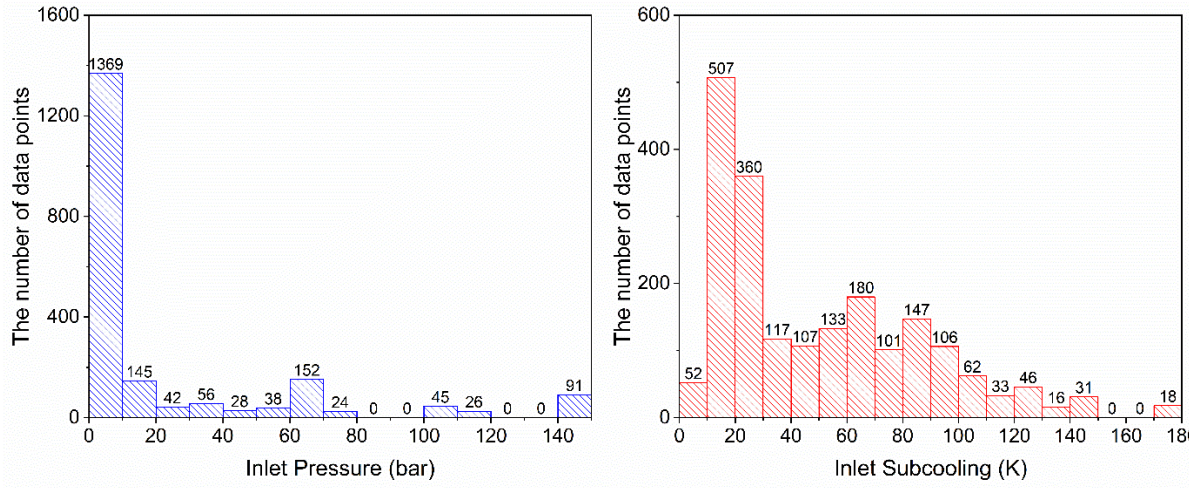

Fig. 5. The distribution of experimental data according to inlet pressure and inlet subcooling

V. CONCLUSIONS

The study conducted to collect experimental data on subcooled boiling flow, for investigation, and verification different empirical correlations to predict void fraction of subcooled boiling flow in vertical upward channel. Besides, the research also proposes the use of data-driven model based on ANN, which provides better predictive performance than empirical correlations. The results clearly show the possibility that the ANN-based model can be used in predicting the parameters of the two-phase flows. The study is the first step to build the ANN-based model to replace mathematical models implemented in CFD codes.

ACKNOWLEDGEMENT

This research is funded by the Hanoi University of Science and Technology (HUST) under project number T2020-PC-059.

REFERENCES

[1]. Y. Liu, N Dinh, Y Sato. B Niceno. "Data-driven modeling for boiling heat transfer: using deep neural networks and high-fidelity simulation results", *Applied Thermal Engineering*, 144(5), 2018.

[2]. S. Azizi et al., "Prediction of void fraction for gas-liquid flow in horizontal, upward and downward inclined pipes using artificial neural network", *International Journal of Multiphase Flow*, 87, 2016.

[3]. G. Su et al., "Applications of artificial neural network for the prediction of flow boiling curves", *Journal of Nuclear Science and Technology*, 39(11), 2002.

[4]. N. Bar et al., "Prediction of frictional pressure drop using Artificial Neural Network for air-water flow through U-bend", *International Conference on Computational Intelligence: Modeling Techniques and Applications (CTMTA)*, 2013.

[5]. X. Liang et al., "A data driven deep neural network model for predicting boiling heat transfer in helical coils under high gravity", *Journal of Heat and Mass Transfer*, 166, 2021.

[6]. C. Cai et al., "Assessment of void fraction models and correlations for subcooled boiling in vertical upflow in circular tube", *International Journal of Heat and Mass Transfer*, 171, 2021.

[7]. J.K. Ferrell (1964), "*A study of convection boiling inside channels*", Raleigh, North Carolina, US.

[8]. S.Z. Rouhani (1966), "*Void measurements in the regions of subcooled and low quality boiling, Part 2. Higher Mass Velocities*", Stockholm, Sweden.

[9]. O.M. Zeitoun (1994), "*Subcooled Flow Boiling and Condensation*", Ph. D Thesis, McMaster University, Canada.

[10]. A.S. Devkin, A.S. Podosenov (1998), "*RELAP5/MOD3 Subcooled boiling model assessment*", U.S Nuclear Regulatory Commission, United States.

[11]. R. Situ et al., "Axial development of subcooled boiling flow in an internally heated annulus", *Experiments in Fluids*, 37, 589-603, 2004.

[12]. T.H. Lee et al., "Axial developments of interfacial area and void concentration profiles in subcooled boiling flow of water", *International Journal of Heat and Mass Transfer*, 52, 473-487, 2009.

[13]. B.J. Yun et al., "Characteristics of the local bubble parameters of a subcooled boiling flow in an annulus", *Nuclear Engineering and Design*, 240, 2010.

[14]. B.J. Yun et al., "Experimental investigation of local two-phase flow parameters of a subcooled boiling flow in an annulus", *Nuclear Engineering and Design*, 240, 2010.

[15]. T.H. Lee et al., "Local interfacial structure of subcooled boiling flow in a heated annulus", *Journal of Nuclear Science and Technology*, 45(7), 683-697, 2012.

[16]. B. Ozar et al., “Interfacial area transport of vertical upward stream-water two-phase flow in an annular channel at elevated pressures”, *International Journal of Heat and Mass Transfer*, 57, 504-518, 2013.

[17]. C.S. Brooks et al., “Interfacial area transport of subcooled boiling flow in a vertical annulus”, *Nuclear Engineering and Design*, 268, 152-163, 2014.

[18]. G.E. Dix (1971), “*Vapor void fractions for forced convection with subcooled boiling at low flow rates*”, Ph. D Thesis, University of California, United States.

[19]. P. Saha, N. Zuber, “Point of net vapor generation and vapor void fraction in subcooled boiling”, *International Heat Transfer Conference Digital Library*, 4, 175-179, 1974.

[20]. T.W. Ha et al., “Improvement of the subcooled boiling model for thermal-hydraulic system codes”, *Nuclear Engineering and Design*, 364, 2020.

[21]. S.Y. Ahmad, “Axial distribution of bulk temperature and void fraction in a heated channel with inlet subcooling”, *Journal of Heat Transfer*, 70, 1970.

[22]. N. Zuber, J. Findlay, “Average volumetric concentration in two-phase flow systems”, *Journal of Heat Transfer*, 87, 453-468, 1965.

[23]. T. L. Cong et al., “Applications of ANNs in flow and heat transfer problems in nuclear engineering: a review work”, *Progress in Nuclear Energy*, 62, 54-71, 2013.

[24]. N. D. Nguyen, V. T. Nguyen, “Development of ANN structural optimization framework for data-driven prediction of local two-phase flow parameters”, *Progress in Nuclear Energy*, 146, 104176, 2022.

[25]. P. Benardos and G. Vosniakos, “Optimizing feedforward artificial neural network architecture”, *Engineering Applications of Artificial Intelligence*, 20(3), 365-382, 2007.